Generating Molecular Rovibrational Coherence by Two-Photon Femtosecond Photoassociation of Thermally Hot Atoms

Leonid Rybak,[1] Saieswari Amaran,[2] Liat Levin,[1] Michał Tomza,[3] Robert Moszynski,[3] Ronnie Kosloff,[2] Christiane P. Koch,[4,5] and Zohar Amitay[1,*]

[1] *The Shirlee Jacobs Femtosecond Laser Research Laboratory, Schulich Faculty of Chemistry, Technion-Israel Institute of Technology, Haifa 32000, Israel*
[2] *Institute of Chemistry, Hebrew University, Jerusalem 91904, Israel*
[3] *Department of Chemistry, University of Warsaw, Pasteura 1, 02-093 Warsaw, Poland*
[4] *Institut für Theoretische Physik, Freie Universität Berlin, Arnimallee 14, 14195 Berlin, Germany*
[5] *Theoretische Physik, Universität Kassel, Heinrich-Plett-Str. 40, 34132 Kassel, Germany*

The formation of diatomic molecules with rotational and vibrational coherence is demonstrated experimentally in free-to-bound two-photon femtosecond photoassociation of hot atoms. In a thermal gas at a temperature of 1000 K, pairs of magnesium atoms, colliding in their electronic ground state, are excited into coherent superpositions of bound rovibrational levels in an electronically excited state. The rovibrational coherence is probed by a time-delayed third photon, resulting in quantum beats in the UV fluorescence. A comprehensive theoretical model based on *ab initio* calculations rationalizes the generation of coherence by Franck-Condon filtering of collision energies and partial waves, quantifying it in terms of an increase in quantum purity of the thermal ensemble. Our results open the way to coherent control of a binary reaction.

When a pair of colliding atoms is irradiated by a femtosecond pulse, an important scenario is photoassociation (PA) in which a chemical bond is "photo-catalysed" via a free-to-bound broadband optical transition [1–6]. Femtosecond laser pulses can be shaped in their amplitude, phase and polarization. They are thus the basic tool for coherent control which employs interference of matter waves to steer the dynamics of a quantum system toward a desired outcome [7–9]. Chemical reaction control, as a means for photo-inducing new chemical synthesis, is a long-standing yet unrealized goal from the early days of coherent control [8]. While coherent control has been extremely successful for destructive unimolecular processes such as ionization or dissociation [10–14], control of associative binary reactions still remains an unresolved puzzle. A controlled photoassociation step between two atoms or two molecules has been proposed as a first step in an extended control scheme of more complicated bimolecular reactions [15]. Femtosecond photoassociation leading to chemical bond formation is thus the prerequisite for coherent control of a binary reaction. Femtosecond photoassociation of hot atoms (hot fs-PA) has been demonstrated in a single pioneering experimental study more than 15 years ago [1], using mercury and a single-photon UV transition. Coherent rotational molecular dynamics were observed following the PA. In order to utilize hot fs-PA as a basis for coherent control of binary reactions, it is, however, essential to induce *vibrational* coherence of the photoassociated molecules since the vibrational degrees of freedom determine the fate of bond making and breaking. In view of a large control toolbox, it would be optimal to have both one-photon and multi-photon fs-PA available. The high peak powers of femtosecond laser pulses can easily drive multi-photon transitions, resulting in a large range of molecular excitation energies amenable to fs-PA. Multi-photon PA allows for accessing electronically excited molecular states that are inaccessible in one-photon PA due to the different selection rules. It also allows for utilizing multi-photon control strategies that differ from one-photon control strategies due to an extended manifold of state-to-state quantum pathways and large non-resonant Stark shifts [16]. Moreover, in view of experimental feasibility, fs-PA using non-resonant multi-photon transitions with near-IR or visible photons is desirable in order to associate molecules which have their lowest electronic transition in the deep-UV or VUV spectral range where pulse shaping is more difficult. Multi-photon fs-PA thus extends the variety of molecular species and reactions that are candidates for coherent control using shaped pulses.

In this Letter, we demonstrate two-photon hot fs-PA with subsequent coherent molecular motion that is of both rotational and vibrational nature. Our experimental and theoretical results are presented for fs-PA of hot magnesium atoms into bound magnesium dimer molecules, i.e., $Mg+Mg \rightarrow Mg_2^*$, with the thermal ensemble of Mg atoms held at a temperature of 1000 K. We show that femtosecond laser pulses can carve from an initial incoherent mixture a sub-ensemble with increased quantum purity, $\mathsf{Tr}[\hat{\boldsymbol{\rho}}^2]$, and dynamical coherences that are amenable to coherent control.

Magnesium is experimentally well-suited for PA studies for two main reasons. (i) The experimental background signal originating from direct bound-bound optical excitation of already-bound ground-state dimers is very small. This is due to the van der Waals nature of the molecular ground electronic state whose shallow well of only about 400 cm^{-1} is outweighted by the rotational barrier and does not support any bound states for most of the thermally populated partial waves. (ii)

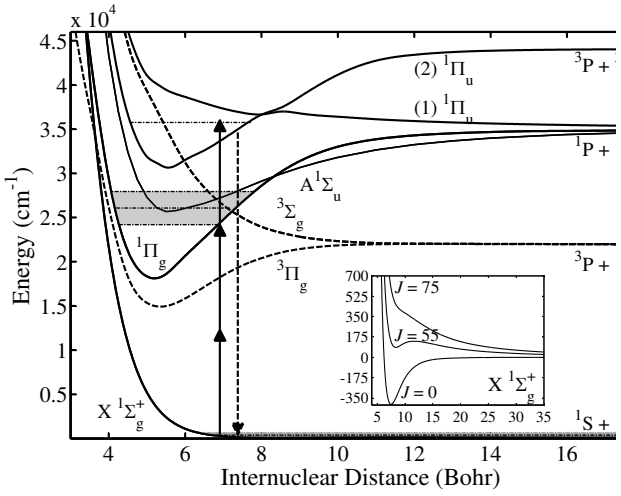

FIG. 1: The excitation scheme of the two-photon femtosec photoassociation of magnesium. The shaded areas indicate the thermally populated scattering states in the electronic ground state and the vibrational band of Π_g-state molecules inferred from the autocorrelation function. The position of the vibrational band *above* the weak-field two-photon resonance is rationalized by the strong dynamical Stark shift.

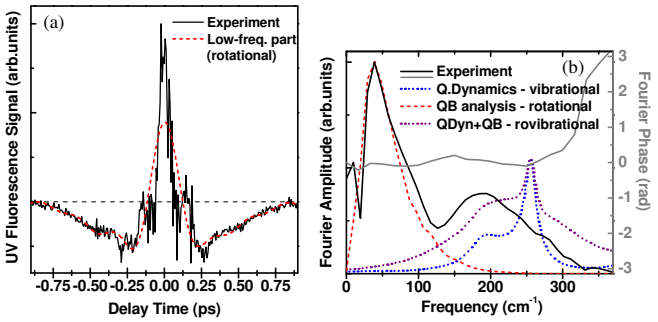

FIG. 2: (color online) Two-photon femtosecond photoassociation of hot magnesium atoms: (a) Experimental pump-probe signal showing the measured UV fluorescence intensity as a function of the pump-probe delay (black line). The red line corresponds to rotational dynamics only. It results from a low-pass step filter set to include only frequencies smaller than 4 THz or 133.42 cm^{-1}. (b) Fourier spectrum of the experimental pump-probe trace (solid black and grey lines). Superimposed are the theoretical amplitude spectra corresponding to purely vibrational dynamics (blue dotted line), purely rotational dynamics (dashed red line) and vibrational dynamics including rotational broadening (purple dotted line).

The electronically excited states of Mg_2 with deep potential wells are conveniently accessible in a free-to-bound PA process via optical transitions of two or three NIR photons. Figure 1 displays the relevant Mg_2 potential energy curves and the present excitation scheme. The inset of the figure shows the ground $X^1\Sigma_g^+$ state for three different values of partial waves, J, of the colliding Mg atoms: Already for $J \approx 50$, the X-state does not support any bound levels. The temperature of $T = 1000\,\mathrm{K}$ corresponds to a collision energy $k_BT/2$ of $\sim 350\,\mathrm{cm}^{-1}$. Pairs of Mg atoms colliding in the $X^1\Sigma_g^+$ electronic ground state of Mg_2 are excited via a broadband free-to-bound non-resonant two-photon transition into coherent superpositions of bound rovibrational levels in the electronically excited $(1)^1\Pi_g$ state. The non-resonant two-photon coupling is provided by off-resonant dipole transitions to intermediate states of *ungerade* symmetry with the largest contribution coming from the lowest states, $A^1\Sigma_u^+$, $(1)^1\Pi_u$ and $(2)^1\Pi_u$. PA is induced by pulses of 70 fs transform-limited duration, 840 nm central wavelength, linear polarization, and a transform-limited peak intensity of about 5×10^{12} W/cm^2. A time-delayed probe pulse, identical to the pump pulse, probes the dynamics of the excited dimers via a one-photon excitation to the higher lying $(1)^1\Pi_u$ electronic state. This state has a strong one-photon allowed transition to the $X^1\Sigma_g^+$ ground state with a lifetime of a few ns. The intensity of the resulting UV fluorescence at 285-292 nm is measured as a function of the pump-probe time delay τ, yielding the pump-probe signal transient. The experiments are conducted in a static cell with argon buffer gas and a pressure of the Mg vapor of ~ 5 Torr. The sample is irradiated at a repetition rate of 1 kHz by the pump and probe laser beams. UV fluorescence emitted toward the laser-beam entrance to the cell is collected at a small angle from the laser-beam axis using an appropriate optical setup.

Figure 2 presents experimental results for two-photon fs-PA of hot magnesium atoms, showing the measured pump-probe transient in Fig. 2(a) and its Fourier Transform (FT) spectrum in Fig. 2(b). The time-dependent pump-probe transient signal, symmetric around $\tau = 0$ since pump and probe pulses are identical, is observed also for delay times where the photoassociating pump pulse has already ended. As corroborated by the calculations presented below, observation of this time-dependence demonstrates that (i) molecules have been formed in a non-stationary coherent state, i.e., in a coherent superposition of molecular rovibrational states, and (ii) the generated ensemble of photoassociated molecules must be of increased purity as compared to the initial thermal, incoherent atomic ensemble – without an increase in purity, no coherence could be observed. The FT spectrum of the experimental pump-probe signal, cf. Fig. 2(b), is composed of a narrow low-frequency peak at around 38.9 cm^{-1} and a broad high-frequency peak located at 189.6 cm^{-1}. It shows a zero spectral phase, confirming that pump and probe excitation occur at the same R, cf. Fig. 1. Below, we show the low-frequency peak to be associated to coherent rotational dynamics and the high-frequency peak to coherent vibrational dynamics.

To interpret the experimental data, we have con-

structed a comprehensive theoretical model. State-of-the-art *ab initio* methods have been employed to calculate the Mg_2 potential energy curves presented in Fig. 1 as well as the corresponding one-photon and two-photon transition dipole moments, dynamical Stark shifts, and spin-orbit interaction, non-adiabatic and radial couplings in the electronically excited states. The short-range part of the potentials and transition moments were calculated within the framework of the equation of motion (reponse) coupled cluster method restricted to single and double excitations [17, 18] in a large basis set. The long-range part of the potentials as well as the non-adiabatic, radial and spin-orbit couplings have been obtained using multi-reference configuration interaction. A high accuracy of the computed potential energy curves is confirmed by a good agreement of the calculated spectroscopic constants with their experimental values. Our *ab initio* data are by far much more accurate than previous results reported in Refs. [19]. The PA dynamics are simulated non-perturbatively by solving the time-dependent Schrödinger equation on a multi-surface grid including all non-adiabatic couplings and one-photon and two-photon transition dipole operators. It is crucial to correctly represent the initial thermal ensemble of scattering atoms (as opposed to a single state which is always coherent). The incoherent initial state is described by the density operator in the canonical ensemble, $\hat{\boldsymbol{\rho}}(t=0) = \exp[-\beta\hat{\mathbf{H}}_g]/Z$ with $\beta = 1/k_BT$, $\hat{\mathbf{H}}_g$ the Hamiltonian for nuclear motion in the ground electronic state, and Z the partition function, $Z = \mathsf{Tr}[\exp[-\beta\hat{\mathbf{H}}_g]]$ It is constructed using random-phase wavefunctions [20]. Details of the electronic structure calculations and the random-phase thermal wavefunction approach are reported elsewhere [21].

Separating rotational and vibrational motion, the PA dynamics is simulated by propagating many realizations of random-phase thermal wavefunctions under the pump and probe pulses for each value, J, of the incoming partial waves. Computing the expectation value of an observable for each propagated random-phase wavefunction and incoherently summing all individual expectation values yields the thermally averaged time-dependent expectation value. For example, the calculated spectrum shown in Fig. 2(b) (blue dotted line) is obtained by Fourier transforming the thermally averaged time-dependent population of the $^1\Pi_u$ states. Since the full pump-probe simulation for many random-phase realizations and all thermally populated partial waves J is numerically rather demanding, our calculations account only for optical transitions of $\Delta J = 0$. Our quantum dynamical results therefore reflect the dependence of hot fs-PA on the partial waves, J, but the calculated dynamics is of purely *vibrational* nature.

Comparing the experimental spectrum to the calculated one (black solid and blue dashed lines in Fig. 2(b)), we find the high-frequency peak to be due to coherent vibrational dynamics. The range of populated vibrational levels in the $^1\Pi_g$ state is indicated by the grey shaded area in Fig. 1. We approximately account for the rotational dynamics by carrying out a quantum-beat analysis: We assume rovibrational $^1\Pi_g$ levels with $J' = J, J\pm1, J\pm2, J\pm3, J\pm4$ to get excited by the pump pulse from each incoming partial wave J. Each pair of rovibrational $^1\Pi_g$ levels, (v_1', J_1'), (v_2', J_2'), with $v_2' = v_1', v_1'+1$ and $|J_2' - J_1'| = 2, 4$ contributes to the FT spectrum an amplitude $P_{^1\Pi_g}(J)$ at the frequency $\omega_{QB} = (E_{v_1',J_1'} - E_{v_2',J_2'})/\hbar$. $P_{^1\Pi_g}(J)$ is the $^1\Pi_g$ state population obtained in the vibrational dynamics simulation for each incoming J, shown in Fig. 3(a). The result of the quantum-beat analysis is shown by the red dashed line in Fig. 2(b) and describes the low-frequency peak in the experimental spectrum very well. We thus find this peak to fit pairs of $^1\Pi_g$ levels with $v_1' = v_2'$ and $J_1', J_2' \approx 40\ldots100$. In particular, the quantum beat frequency corresponding to the maximum of the peak matches only pairs with $J_{1,2}' \approx 50\ldots60$. Combining our approximate treatment of the rotational dynamics with the full quantum simulation of the vibrational dynamics leads to rotational broadening of the vibrational peak, cf. purple dotted line in Fig. 2(b). We attribute the remaining small discrepancy between the experimental and the theoretical spectrum to the separation of rotational and vibrational dynamics and the uncertainty of the *ab initio* calculations. In particular, the sharp feature in the calculated vibrational spectrum is due to the non-adiabatic couplings between the $^1\Pi_u$ states which carry the largest error bar of the otherwise very accurate *ab initio* results. To summarize, the peaks observed in the experimental spectrum originate from coherent excitation and probing of pairs of rovibrational levels (v_1', J_1') and (v_2', J_2') with high rotational quantum numbers in the $(1)^1\Pi_g$ electronically excited state.

As illustrated in the inset of Fig. 1, for values of $J \gtrsim 50$, the $X^1\Sigma_g^+$ ground state of Mg_2 does not support any bound molecular level. We therefore deduce from our quantum beat analysis that indeed the majority of the bound excited Mg_2 molecules, that we probe experimentally, have been generated in a free-to-bound coherent PA process. This conclusion of free-to-bound PA of high-J molecules is further supported by the calculated relative PA probabilities, shown in Figure 3(a), as a function of the incoming partial wave, J. Maximum PA probability is observed for $J = 55$, for which the electronic ground state does not support bound levels, cf. Fig. 1. A careful analysis shows that about 80 per cent of the total signal is due to free-to-bound PA [21].

In order to rationalize and quantify the generation of the coherence, that is observed in Fig. 2, out of a completely incoherent initial ensemble, we consider the change in quantum purity, $\mathsf{Tr}[\hat{\boldsymbol{\rho}}^2]$, due to the femtosecond laser pulses. The initial purity, determined by the temperature, $T = 1000\,\mathrm{K}$, and density, $\rho =$

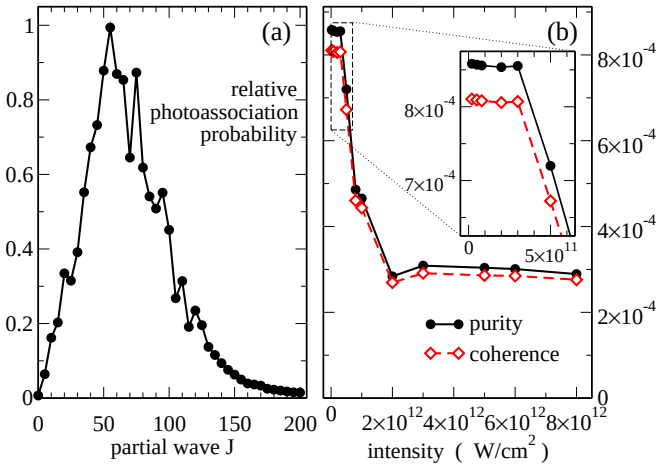

FIG. 3: (a) Calculated relative PA probability as a function of incoming partial wave J. (b) Quantum purity, $\mathsf{Tr}[\hat{\boldsymbol{\rho}}(t_{final})^2]$ and dynamical coherence of the sub-ensemble of molecules in the $(1)^1\Pi_g$ state vs laser intensity

$4.8 \cdot 10^{16}$ atoms/cm^3, of the experiment, is estimated in terms of the purity of a single atom pair represented in our computation and the probability, p_2, of finding two atoms in our computation volume, $\mathcal{V}$. Given ρ and $\mathcal{V} = 4/3\pi r^3 = 6.33{\cdot}10^{-21}$ cm^3, we find $p_2 = 9.2{\cdot}10^{-8}$. The purity of a single atom pair in our computation box is given by the vibrational purity weighted by the probability, P_J, for occupation of the sub-ensemble with angular momentum J. For an atom pair in their electronic ground state, the purity becomes $\mathcal{P}^g = p_2^2 \sum_J P_J^2 \mathcal{P}_J^g$ where $\mathcal{P}_J^g = \mathsf{Tr}[(e^{-\beta \hat{\mathbf{H}}_g^J})^2]/Z_J^2$, and $\hat{\mathbf{H}}_g^J$ and Z_J are the Hamiltonian for vibrational motion and partition function, respectively, of partial wave J. Evaluating $\mathcal{P}_J^g$ with thermal random-phase wavefunctions, we obtain $\mathcal{P}^g = 2.6 \cdot 10^{-20}$ for the initial purity. For the ensemble of molecules in the electronically excited $^1\Pi_g$ state, the density operator is given by $\hat{\boldsymbol{\rho}}^e = \sum_J P_J^e \hat{\boldsymbol{\rho}}_J^e$. Here, P_J^e is the probability for occupation of the excited state sub-ensemble with angular momentum, J, cf. Fig. 3(a). $\hat{\boldsymbol{\rho}}_J^e$ is the normalized density operator of the excited state J sub-ensemble which is constructed by incoherently averaging dyadic products of the propagated thermal wavefunctions, $|\psi_{n,J}(t_{final})\rangle\langle\psi_{n,J}(t_{final})|$, over all random phases n and partial waves J (t_{final} denotes the time when the pump pulse is over). The purity for the excited state sub-ensemble is then given by $\mathcal{P}^e = \sum_J (P_J^e)^2\, \mathsf{Tr}[(\hat{\boldsymbol{\rho}}_J^e)^2]$. We obtain a purity $\mathcal{P}^e = 3.04 \cdot 10^{-4}$ for the molecular sub-ensemble in the $^1\Pi_g$ excited state for the experimental pulse parameters. We thus observe a dramatic increase in the quantum purity, $\mathsf{Tr}[\hat{\boldsymbol{\rho}}^2]$, induced by the femtosecond laser pulse. The underlying physical mechanism can be viewed as "Franck-Condon filtering": for a given initial J value there is only a limited range of collision energies that allow the colliding pair to reach the Franck-Condon window for PA located at short internuclear distances [2].

In order to obtain a quantitative estimate of the degree of distillation achieved by the fs-PA process, we have calculated the purity of ensemble of photoassociated molecules in the $^1\Pi_g$ state for a range of laser intensities, cf. Fig. 3(b). For weak fields, the purity is roughly constant as a function of intensity and almost three times larger than the purity obtained for the intensity of 5×10^{12} W/cm^2 used in the experiment. As intensity is increased, a sudden drop in the purity is observed which levels off at large intensities. We attribute this drop to power broadening for strong fields, which brings more atom pairs into the Franck-Condon window for PA. The purity increase with respect to the initial ensemble is nevertheless many orders of magnitude for both weak and strong field. To further analyze the generation of quantum coherence, it is possible to separate static and dynamic contributions, $\hat{\boldsymbol{\rho}} = \hat{\boldsymbol{\rho}}_{stat} + \hat{\boldsymbol{\rho}}_{dyn}$. This is most easily achieved in the energy representation where the static (dynamic) part corresponds to the diagonal (off-diagonal) matrix elements. The dynamical contributions are quantified by the coherence measure $\mathcal{C} = \mathsf{Tr}[\hat{\boldsymbol{\rho}}_{dyn}^2(t)] < \mathsf{Tr}[\hat{\boldsymbol{\rho}}^2(t)]$ [22]. Tracing the coherence measure of the excited state, $\mathcal{C}^e$, as a function of laser intensity (red open diamonds in Fig. 3(b)) shows that most of the purity comes from the dynamical contribution ($\mathcal{C}^e = 2.86 \cdot 10^{-4}$ for $I = 5 \times 10^{12}$ W/cm^2).

In summary, we have demonstrated femtosecond photoassociation of hot atoms using non-resonant two-photon transitions driven by NIR light. Quantum beats in the observed UV fluorescence reflect both vibrational and rotational coherence of the photoassociated molecules. Our experiment is the first to demonstrate generation of vibrational coherence in a light-induced binary reaction. This is rationalized by our theoretical model in terms of Franck-Condon filtering, yielding an increased quantum purity of the sub-ensemble of the reaction products, the photoassociated molecules, as compared to that of the reaction partners, the atoms. Vibrational coherence is a prerequisite for further control of the reaction products. Our work thus opens the way toward coherent control of a binary reaction.

This research was supported by The Israel Science Foundation (grant No. 1450/10), The James Franck Program in Laser Matter Interaction, the Polish Ministry of Science and Higher Education (project N N204 215539), the Foundation for Polish Science MPD Programme co-financed by the EU European Regional Development Fund, and the Deutsche Forschungsgemeinschaft.

* Electronic address: amitayz@tx.technion.ac.il

[1] U. Marvet and M. Dantus, Chem. Phys. Lett. **245**, 393 (1995).
[2] P. Backhaus and B. Schmidt, Chem. Phys. **217**, 131 (1997).

[3] A. Vardi, D. Abrashkevich, E. Frishman, and M. Shapiro, J. Chem. Phys. **107**, 6166 (1997).

[4] M. Bonn et al., Science **285**, 1042 (1999).

[5] W. Salzmann et al., Phys. Rev. Lett. **100**, 233003 (2008).

[6] P. Nuernberger, D. Wolpert, H. Weiss, and G. Gerber, Proc. Natl. Acad. Sci. USA **107**, 10366 (2010).

[7] S. A. Rice and M. Zhao, *Optical control of molecular dynamics* (John Wiley & Sons, 2000).

[8] P. Brumer and M. Shapiro, *Principles and Applications of the Quantum Control of Molecular Processes* (Wiley Interscience, 2003).

[9] C. Brif, R. Chakrabarti, and H. Rabitz, New J. Phys. **12**, 075008 (2010).

[10] R. J. Gordon and S. A. Rice, Annu. Rev. Phys. Chem. **48**, 601 (1997).

[11] T. Brixner and G. Gerber, ChemPhysChem **4**, 418 (2003).

[12] M. Dantus and V. V. Lozovoy, Chem. Rev. **104**, 1813 (2004).

[13] M. Wollenhaupt, V. Engel, and T. Baumert, Annu. Rev. Phys. Chem. **56**, 25 (2005).

[14] O. Kühn and L. Wöste, eds., *Analysis and control of ultrafast photoinduced reactions* (Springer, Berlin, 2007).

[15] R. Kosloff, S. Rice, P. Gaspard, S. Tersigni, and D. Tannor, Chem. Phys. **139**, 201 (1989).

[16] Y. Silberberg, Annu. Rev. Phys. Chem. **60** (2009).

[17] H. Sekino and R. J. Bartlett, Int. J. Quantum Chem. Symp. **18**, 255 (1984).

[18] H. Koch and P. Jørgensen, J. Chem. Phys. (1990).

[19] E. Czuchaj, M. Kronicki, and H. Stoll, Theor. Chem. Acc. **107**, 27 (2001).

[20] D. Gelman and R. Kosloff, Chem. Phys. Lett. **381**, 129 (2003).

[21] S. Amaran, R. Kosloff, M. Tomza, R. Moszynski, L. Rybak, Z. Amitay, and C. P. Koch, in preparation.

[22] U. Banin, A. Bartana, S. Ruhman, and R. Kosloff, J. Chem. Phys. **101**, 8461 (1994).